All-*trans* retinoic acid (ATRA) induced *TFEB* expression is required for myeloid differentiation in acute promyelocytic leukemia (APL)

Short running title: ATRA-induced APL differentiation requires TFEB

Nina Orfali[1,2,3.*], Tracey R. O'Donovan[1,*], Mary R. Cahill[1,2], Dalyia Benjamin[1,2,3], David M. Nanus[4], Sharon L. McKenna[1, 6], Lorraine J. Gudas[3,6], and Nigel P. Mongan[3,5,6]

1. Cork Cancer Research Centre & CancerResearch@UCC, Western Gateway Building, University College Cork, Cork, Ireland
2. Department of Haematology, Cork University Hospital, Wilton, Cork, Ireland
3. Department of Pharmacology, Weill Cornell Medicine, New York, NY 10065, USA
4. Division of Hematology and Medical Oncology, Department of Medicine, Weill Cornell Medicine, New York, NY 10065, USA
5. Faculty of Medicine and Health Science, School of Veterinary Medicine and Science, University of Nottingham, Sutton Bonington, United Kingdom

*Joint first authors

Authors for correspondence[6]

Dr. Nigel P. Mongan,	Dr. Lorraine J. Gudas,	Dr. Sharon L. McKenna
Faculty of Medicine and	Department of	Cork Cancer Research Centre
Health Science,	Pharmacology	& CancerResearch@UCC,
University of Nottingham,	Weill Cornell Medicine,	University College Cork,
Sutton Bonington, UK	New York, NY, USA	Cork, Ireland
nigel.mongan@nottingham.ac.uk	ljgudas@med.cornell.edu	s.mckenna@ucc.ie

Conflict-of-interest disclosure: The authors declare no competing financial interests.

Trial registration: clinicaltrials.gov identifier: NCT00195156

Abstract

Objective

In acute promyelocytic leukemia (APL), normal retinoid signaling is disrupted by an abnormal PML-RARα fusion oncoprotein, leading to a block in cell differentiation. Therapeutic concentrations of all-*trans*-retinoic acid (ATRA) can restore retinoid-induced transcription and promote degradation of the PML-RARα protein. Autophagy is a catabolic pathway that utilizes lysosomal machinery to degrade intracellular material and facilitate cellular re-modelling. Recent studies have identified autophagy as an integral component of ATRA-induced myeloid differentiation.

Methods

As the molecular communication between retinoid signaling and the autophagy pathway is not defined, we performed RNA sequencing of NB4 APL cells treated with ATRA and examined autophagy-related transcripts.

Results

ATRA altered the expression of >80 known autophagy-related transcripts, including the key transcriptional regulator of autophagy and lysosomal biogenesis, *TFEB* (11.5-fold increase). Induction of *TFEB* and its transcriptional target, sequestosome 1 (*SQSTM1, p62),* is reduced in ATRA-resistant NB4R cells compared to NB4 cells. *TFEB* knockdown in NB4 cells alters the expression of transcriptional targets of TFEB and reduces *CD11b* transcript levels in response to ATRA.

Conclusions

We show for the first time that TFEB plays an important role in ATRA-induced autophagy during myeloid differentiation, and that autophagy induction potentiates leukemic cell differentiation. (Note: this study includes data obtained from NCT00195156, https://clinicaltrials.gov/show/NCT00195156).

Abstract word count = 200

Word count (text) = 5,434

References = 50

Figures = 6

Supplemental Figures = 4

Supplemental Tables = 4

Introduction

Retinoids are signaling molecules related to Vitamin A (retinol) that have well-established roles in development and differentiation.[1] Dietary retinoids are metabolized within cells to a bioactive form, all-*trans*-retinoic acid (ATRA), which exerts its effects by mediating gene transcription.[1] ATRA binds retinoic acid receptors (RARs) and rexinoid receptors (RXRs). These ligand-dependent transcription factors form RXR-RAR heterodimers that preferentially bind to specific DNA sequence motifs, termed retinoic acid response elements (RAREs), in the promoters or enhancers of target genes.[1] Through interactions with diverse, co-regulatory proteins the RXR-RAR complexes regulate transcription.[2]

Acute promyelocytic leukemia (APL), a distinct subtype of acute myeloid leukemia (AML), is defined by the clonal proliferation of granulocyte precursors halted at the promyelocyte stage of development.[3] Cytogenetically, APL is distinguished by a chromosomal translocation affecting the *RARα* gene locus on chromosome 17q21 in malignant clones,[4] most commonly generating the functional *PML-RARα* fusion oncogene.[4] The PML-RARα oncoprotein binds to RAREs on retinoid target gene promoters. Because of its high affinity for co-repressor protein complexes, PML-RARα causes repressive epigenetic changes that inhibit the transcription of RARα target genes, many of which are involved in myeloid differentiation.[5-7] While physiologic concentrations of ATRA (~1 nM) are unable to overcome this transcriptional repression, therapeutic concentrations (~1 μM) restore granulocytic differentiation in leukemic cells, allowing them to complete a finite life cycle.[6] The incorporation of ATRA into clinical regimens has transformed outcomes for APL patients, with cure rates of >80% now observed.[8] Recent data show that ATRA has a dual therapeutic effect on the PML-RARα oncoprotein: (i) it induces a conformational change in the oncoprotein that results in the dissociation of co-repressor proteins and allows the preferential binding of transcriptional co-activators, and (ii) it promotes the degradation of the PML-RARα oncoprotein through co-operating proteolytic

mechanisms.[4,9] This oncoprotein elimination, particularly in leukemia-initiating cells, results in sustained clinical responses.[9] Recently, ATRA-induced differentiation has been shown to involve the induction of autophagy.[10-13]

Autophagy is a constitutive pathway involved in the turnover of damaged or redundant proteins.[14,15] The core machinery of autophagy is largely comprised of 'AuTophaGy-related' (ATG) proteins, which through a series of conjugation reactions are sequentially recruited to regulate autophagosome formation and fusion.[16] While initially described as a non-specific degradation pathway, substrate selectivity in autophagy is achieved via adaptor proteins such as sequestosome1 (SQSTM1/p62) and NBR1.[17,18] The regulation of autophagy is complex and occurs at cytoplasmic and transcriptional levels. The serine/threonine kinase mammalian target of rapamycin (mTOR) acts as a master cytoplasmic regulator of autophagy.[18] Further cytoplasmic regulation is provided by adenosine monophosphate-activated protein kinase (AMPK) and myo-inositol-1,4,5-triphosphate (IP_3) signaling.[19]

The basic helix-loop-helix leucine zipper transcription factor EB (TFEB) promotes the transcription of a gene network that co-ordinates both autophagy and lysosomal biogenesis.[20,21] Under basal conditions, TFEB is phosphorylated by mTOR and retained at the lysosome.[22] Following autophagy activation TFEB is dephosphorylated and enters the nucleus to exert its transcriptional effects.[21] Notable autophagy-related TFEB targets include LC3B, SQSTM1/p62, and ATG9B, a critical transmembrane protein in autophagosome membrane assembly.[21]

It is known that ATRA induces autophagy in human APL cells.[10-13] This ATRA-induced autophagy is important for the successful granulocytic differentiation of leukemic blasts.[11,12,23] Indeed, autophagy is likely involved in the degradation of the highly aggregate-prone PML-RARα oncoprotein, a process dependent on the SQSTM1/p62 adaptor protein.[12,13] However, as differentiation involves significant protein remodeling, autophagy may also drive leukemic

differentiation independently of oncoprotein elimination, as it has does in other hematopoietic cell types.[4,11] Thus, the molecular communication between retinoid signaling pathways and autophagy remains poorly understood and is the focus of this study.

Using genome-wide RNA sequencing technology, we examined the changes that occur in autophagy-related genes during ATRA-induced APL differentiation. We show for the first time that *TFEB* mRNA is strikingly increased by ATRA. Furthermore, shRNA-mediated knockdown of *TFEB* in APL cells impeded myeloid differentiation of leukemic cells. Collectively our data implicates TFEB as an important mediator of ATRA-induced differentiation in APL.

Materials and Methods

Cell culture & drug treatments

Cells were cultured as described in Faria *et al.*[24] Valproic acid (1 mM, Sigma-P4543) and arsenic trioxide (0.5 μM, Sigma-A1010) were used. Brefeldin A (Sigma-B7651) was diluted from a 5 mg/ml stock in DMSO to a 10 uM working concentration. BFA was added 24 hours prior to analysis. All-*trans*-retinoic acid (ATRA) (Sigma-R2625) was diluted from a 1 mmol/L stock in 100% ethanol – to 1μM working concentration. The NB4 and ATRA-resistant NB4 lines were described previously.[24,25]

TFEB knockdown cell lines

pLKO.1-puro shRNA vectors targeting *TFEB* (Sigma-TRCN0000437246 = *shTFEB*) or a scrambled off-target control (*shScr*) were transfected into HEK293T cells with lentiviral packaging plasmids pCMVΔ8.9 and pVSVG using Lipofectamine-2000 (Invitrogen-11668). NB4 cells were transduced with supernatant and media containing 20% serum in a 1:1 ratio. Cells then underwent a 10-day selection with puromycin (2 μg/mL) (Sigma-P7255). Two independent TFEB shRNA knockdown NB4 lines were used for some of the analyses shown.

Primary human tissue

Following local research ethics committee approval and informed consent, a pre-treatment bone marrow aspirate and peripheral blood samples were obtained from two patients newly diagnosed with APL. Whole samples were gradient-separated using Histopaque-1077 (Sigma-10771), and a buffy coat of mononuclear cells, comprising predominantly a malignant promyelocyte population, was extracted. We also obtained RNA from peripheral blood mononuclear cells from solid tumor oncology patients treated with ATRA following the approved protocol as part of clinical trial NCT00195156.[26]

RNA extraction, cDNA synthesis, and quantitative real-time (qRT) PCR

Quantitative real-time reverse transcription-PCR was performed.[27] Primers: ***TFEB***:F:5'-AAGCGAGAGCTCACAGATGC-3',R:5'-TGAGGATGGTGCCCTTGTTC-3'; ***p62***:F:5'-CATCGGAGGATCCGAGTGTG-3',R:5'-TTCTTTTCCCTCCGTGCTCC-3'; ***PIK3CD***:F:5'-GGCGGGATGACACTCATTGAT-3',R:5'-GGAAGTCAACCACAACGCTC-3'; ***SIK3***:F:5'-CCAGAGACACCACACGATCC-3',R:5'-AGAACTGCATCCGACATCCG-3'; ***CD11b***:F:5'-ATGGAGTTCAATCCCAGGGAAG-3',R:5'-GAGTCCAGAGCCAGGTCATAAG-3'; ***ATG16L1***:F:5'-GGTCGTGACTTCCTGAGACAAT-3',R:5'-TTGCAAGCCGAATCTGGACTGT-3'; ***CTSD***:F:5'-TGCTCAAGAACTACATGGACGC-3',R:5'-CGAAGACGACTGTGAAGCACT-3'; ***GABARAP***:F:5'-GGGCGAGAAGATCCGAAAGA,R:5'-TCCAGGTCTCCTATCCGAGC-3'; ***GCSFR***:F:5'-AGCATGGGGGGCTCCAGTTTCA,R:5'-ATCCTGGACTGCGTGCCCAAG-3'; ***HPRT***:F:5'-TGCTCGAGATGTGATGAAGG-3',R:5'-TCCCCTGTTGACTGGTCATT-3'.

Gene expression amplicons were validated by sequencing. The transcript levels in biological replicates (n=6) were normalized to *hPRT* levels, and relative differences calculated.[28] Graphical displays and measurements of statistical significance were performed on GraphPad Prism software.

RNA sequencing (RNA-seq) and analysis

Total cellular RNA was extracted using an RNeasy mini-kit (Qiagen-74104) with on-column DNase treatment. For RNA sequencing, two independent biological replicates RNA samples were submitted to the Weill Cornell Genomics Core for quality checks, cDNA library preparation, and sequencing using the Illumina HiSeq-2000 platform. Raw sequence reads in fastq format were aligned to the HG19 genome using Tophat and differentially expressed genes based on calculated RPKM expression values were determined using the Galaxy (http://www.usegalaxy.org) implementation of Cufflinks/Cuffdiff using the Illumina iGenomes HG19 annotation.[29] Unsupervised hierarchical clustering was performed and expression

heatmaps generated from sample RPKM values using Cluster and Treeview software (http://rana.lbl.gov/EisenSoftware.htm). Official gene symbols for transcripts were obtained using Gene ID (http://idconverter.bioinfo.cnio.es) and gene list comparisons were performed using Venny software (http://bioinfogp.cnb.csic.es/tools/venny/). Gene ontology analysis was performed using the Webgestalt server (http://www.webgestalt.org).[30] Raw sequence reads are available in NCBI-GEO database under the accessions: GSE53258 and GSE53259.

Creation of an autophagy/myeloid database

A composite list of 522 autophagy-related human genes was generated from three publicly available autophagy databases: (i) the Human Autophagy Database (www.autophagy.lu), (ii) the Autophagy Database (http://autophagy.info/autophagy/list/GeneList) and (iii) the Autophagy Gene Ontology GO0006914 (www.amigo.geneontology.org) (Supplemental Table 1A). We also generated a list of 217 genes associated with myeloid differentiation comprising known hematopoietic lineage markers such as ITGAM and key hematopoiesis-associated genes sourced from the GO:0030099 gene ontology (Supplemental Table 1B).

ChIP sequencing analysis

We accessed RARα and RNA polymerase II chromatin immunoprecipitation sequencing (ChIP-seq) data from ATRA-treated NB4 (GSE18886)[7] and TSU-1621-MT (GSE60477)[31] cells in WIG format (the summary output post alignment and MACS peak calling) from the NCBI-GEO database. We visualized RARα and RNA polymerase II binding within the *TFEB* and *p62/sqstm1* loci using Integrated Genome Viewer software (https://www.broadinstitute.org/igv/home).

Western blotting

Cellular protein extracts were lysed in modified RIPA buffer (50 mmol/L Tris–HCl, pH 7.4, 150 mmol/L NaCl, 0.25% sodium deoxycholate, 1% IGEPAL, 1 mmol/L EDTA, 1x Pefabloc, 1x Protease inhibitor cocktail, 1 mmol/L Na3VO4, 1 mmol/L NaF). Protein samples were prepared

in NuPAGE LDS Sample buffer (NP008-Invitrogen), separated on NuPAGE 4%–12%, Bis–Tris gels (NP0322-Invitrogen) and electrophoretically transferred onto polyvinyl difluoride membranes (IB401001-Invitrogen). Membranes were incubated with anti-LC3A/B (MBL PD014) antibody diluted 1/1000 in 5% milk overnight, at 4˚C and with anti-β-actin (loading control) (Sigma-A5441) for one hour at room temperature. Proteins were visualized using relevant IR-DYE secondary antibodies (Li-Cor, Cambridge, UK) and quantified on the Odyssey IR imaging system (Li-Cor, Cambridge, UK). For all Western blots, integrated intensities are representative of three independent experiments.

Flow cytometry assays

***Differentiation*.** CD11b live cells were incubated for 45 min with PE-conjugated anti-CD11b antibody (12-0118, eBioscience, UK) in 1% albumin/phosphate-buffered saline and washed with phosphate-buffered saline prior to analysis. An increase in surface expression of CD11b is detected as an increase in fluorescence in the PE channel.

***Autophagy*.** Cells were stained with the Cyto-ID autophagy detection kit (Enzo Life Sciences ENZ-51031-K200) according to the manufacturer's instructions. An increase in the number of autophagic vesicles is detected as an increase in fluorescence in the 488-2 channel.

All data were collected on the BD LSR II flow cytometer with BD FACS Diva acquisition software. Gating and overlay histograms were generated using Flowjo data analysis software.

Results

RNA sequencing of ATRA-treated APL cells confirms activation of a myeloid differentiation program

We and others have recently shown that autophagy plays a role in the NB4 model of APL differentiation.[11] To understand the transcriptional signaling pathways involved we used genome-wide RNA-seq to identify gene expression changes following exposure to therapeutic concentrations of ATRA (1 μM) for 72 hours. As has previously been shown, we morphologically confirmed that ATRA induces differentiation. Untreated NB4 cells have large round nuclei with minimal cytoplasm (Figure 1A). ATRA-treated cells display increased nuclear lobulation and a decreased nuclear to cytoplasmic (N:C) ratio characteristic of maturing granulocytes (Figure 1A). We next extracted RNA from control and ATRA-treated cells at 72 hours and submitted samples from two independent biological repeats for complementary DNA (cDNA) library preparation and RNA sequencing. Differential gene expression analysis, calculated using Cuffdiff, identified 2,598 differentially expressed transcripts comprised of 1,540 upregulated and 1,058 downregulated genes with a significant ($q < 0.05$) and greater than 2-fold change in mRNA expression following ATRA treatment (Supplemental Table 2A). Enrichment analysis showed that many differentially expressed genes grouped to gene ontologies comprising genes in the lysosome and immune response (Supplemental Table 2B).

We examined the transcript changes of 217 genes involved in myeloid differentiation (Supplemental Table 2C). Cufflinks reads per kilobase of exon per million fragments mapped (RPKM) outputs from our duplicate samples were clustered using Cluster 3.0 software, and graphical outputs visualized as heatmaps using TreeView. A magnified section of our heatmap depicts a cluster of key myeloid genes, including *CD11b/ITGAM, CEBPα, CEBPε,* and *GATA2,* with similar patterns of expression (Figure 1B). Overall, we observed a >two-fold increase in the expression of 36 (bold print) and decreased expression of 12 (blue print) myeloid-

differentiation genes (Supplemental Table 2C, bold print). Amongst the ATRA-upregulated genes were those encoding the critical myeloid transcription factors PU.1 (*SP1* gene) and CEBPε (Figure 1B).[32] The GATA2 transcription factor preserves a stem-like state in hematopoietic cells and is downregulated during differentiation.[33] We found that ATRA-treated NB4 cells showed decreased *GATA2* mRNA levels and we observed a similar decrease in transcripts for *MYC*, another transcription factor associated with an undifferentiated state (Figure 1B).[34] We detected a decrease in the transcripts of *CEBP*α, a gene encoding a transcription factor involved in early myeloid differentiation but downregulated during the terminal phase of the process (Figure 1C).[35] The mRNA levels of the *ITGAM* gene encoding CD11b, a frequently used surface marker of myeloid differentiation, were greatly increased (Figure 1B). This finding was validated by quantitative PCR of *ITGAM* transcripts in NB4 cells treated with ATRA or vehicle for 72 hours (Figure 1C). Further qPCR validation of mRNA changes in *CEBP*ε*, PIK3CD, GCSFR, CTSD,* and the differentiation-associated autophagy maker, *GABARAP*[11] confirmed their upregulation following ATRA (Figure 1C-H).

RNA sequencing data indicates ATRA mediates autophagy gene transcription

We examined ATRA-regulated expression changes in autophagy-related genes in NB4 cells by cross-referencing our autophagy gene list with those genes that displayed significant ($q < 0.05$), >2-fold in mRNA levels in our RNA-seq. This identified 2,514 genes differentially expressed genes (DEGs) with ≥2-fold change following ATRA treatment in NB4 cells. Of the 522 members of the composite autophagy-related genes, 84 were also differentially regulated in ATRA-treated NB4 cells (Supplemental Table 2D), consistent with reports linking autophagy and retinoid induced differentiation.[11] Among the mRNAs increased was transcription factor EB (*TFEB*) (+11.5-fold change, $q = 0.00022$), a master transcriptional coordinator of autophagy and lysosomal biogenesis.[36]

To assess whether TFEB, a critical regulator of autophagy, is itself under direct retinoid receptor regulation we interrogated two independent, publicly available RARα AML ChIP-seq datasets (NCBI-GEO:GSE18886,GSE60477) that contain data on the genome-wide distribution of RARα and RNA polymerase II in NB4 and TSU-1621-MT AML cells treated with ATRA for 24 hours.[7,31] RARα and RNA polymerase II bind to the *TFEB* locus in both NB4 and TSU-1621-MT AML cells, suggesting that RARα directly regulates TFEB expression in the presence of ATRA (Figure 2A). We confirmed an ATRA-mediated increase in *TFEB* mRNA in NB4 cells by qRT-PCR (Figure 2B). We detected a 15-fold induction of *TFEB* compared to untreated levels following 72 hours ATRA treatment ($p < 0.0001$). Furthermore *SQSTM1/p62*, a known transcriptional target of TFEB, was also induced by 6-fold ($p < 0.0001$) (Figure 2B,i,ii).[37] This was comparable to a 5.9-fold induction calculated by RNA-seq analysis (Supplemental Table 2A). Our RNA-seq showed an ATRA-induced, 2.1-fold increase in *SIK3* mRNA (Supplemental Table 2A), and we measured a comparable 2.5-fold induction by qPCR ($p < 0.0001$) (Figure 2B,iii).

We then examined whether these genes were induced by ATRA in a differentiation-resistant derivative of NB4 APL cells, NB4R. We observed an ATRA-induction of *TFEB,* but to a lesser degree than that seen in the ATRA-sensitive NB4 cell line (2.5-fold increase) (Figure 2C,i). Similarly, the induction of *SQSTM1/p62* and *SIK3* was impaired in the differentiation-resistant line (Figure 2C,ii,iii), suggesting a role for these genes in leukemic cell differentiation.

We then assessed whether elevation of these autophagy-associated genes could be detected in APL patient cells, treated *ex-vivo* with ATRA. Mononuclear cells separated from the bone marrow of a newly diagnosed APL patient were cultured *ex-vivo* +/- ATRA for 72 hours. *TFEB, SQSTM1/p62*, and *SIK3* were induced to levels comparable to those in NB4 (Figure 2D,i-iii). This induction coincided with increased mRNA levels of *CD11b* and *PIK3CD* (Figure 2D,iv-v),

two genes induced during myeloid differentiation of APL cells (as in Figure 1C,E), confirming *ex vivo* differentiation of these primary patient leukemic cells.

We also analyzed expression of these autophagy-associated genes in cDNA from peripheral blood mononuclear cells (PBMCs) isolated from patients with solid urological tumors that were treated with liposomal ATRA as part of a phase 1/2 clinical trial in 2007.[38] We detected a 2-fold induction of *TFEB* by ATRA in PBMCs from this non-leukemic patient cohort (Supplemental Figure S1).

shRNA-mediated depletion of TFEB impacts ATRA-mediated gene expression in NB4

We then assessed the effects of shRNA-mediated depletion of *TFEB* on the expression of genes regulated by ATRA in NB4 cells. Cells lines expressing either *shTFEB* or a control-targeting sequence in eGFP (*shScr*) were generated by a lentiviral-mediated transduction of NB4 cells. Successful *TFEB* depletion was confirmed by qRT-PCR. ATRA induced a 17-fold increase in *TFEB* mRNA in NB4 cells harboring a non-targeting shRNA, as compared to a 6.7-fold ATRA-induction of *TFEB* in NB4 cells with a shRNA targeting *TFEB* (Figure 3A).

These cell lines were then treated with ATRA or vehicle for 72 hours. RNA sequencing was performed, with two biological repeats, on: (i) vehicle-treated shScramble *(shScr-Ctrl),* (ii) ATRA-treated shScramble (*shScr-ATRA),* (iii) vehicle-treated TFEB-depleted *(shTFEB-Ctrl)* and (iv) ATRA-treated TFEB-depleted *(shTFEB-ATRA).* Cuffdiff analysis of our sequencing data from *shScr-Ctrl* versus *shScr-ATRA* identified 3,916 genes whose transcript levels were altered by ATRA by at least two-fold ($q < 0.05$, with RPKM > 0 in both conditions). Analysis of *shTFEB-Ctrl* versus *shTFEB-ATRA* identified 3,264 genes that were altered by ATRA in the *TFEB*-knockdown population (Supplemental Table 3A-B). Intersection of these two datasets highlighted 1,200 genes with altered expression in *shScr* but not in *TFEB*-depleted cells. Conversely, 548 genes were altered only in the *shTFEB* cells (Figure 3B, Supplemental Table 3C). Another way to state these results is that the comparison of the *shScr* +/- ATRA provides

the number of genes affected by ATRA, 3,916, and the comparison of the *shScr* +/- ATRA and the *shTFEB* + ATRA shows that 1,200 genes, a large number, are regulated by ATRA in the *shScr* but not in the *shTFEB* cells, and thus the expression of these 1,200 genes either directly or indirectly requires expression of TFEB and includes notable components of the autophagy pathway.

TFEB regulates CLEAR network gene expression during ATRA-induced differentiation of APL cells

TFEB is a master regulator of a gene network that controls both autophagy and lysosomal biogenesis, known as the Coordinated Lysosomal Expression and Regulation (CLEAR) network.[39] This includes a network of 471 genes reported to be direct transcriptional targets of TFEB.[21] We examined *TFEB* expression and the TFEB-regulated CLEAR genes in our data-set, comparing vehicle and ATRA-treated *shScr* and *shTFEB* cells (Supplemental Table 4A). Using hierarchical clustering we visualized expression of a subset of CLEAR-network genes in ATRA-treated *shScr* and ATRA-treated *shTFEB* cells (Figure 3C). This analysis of the gene cluster, which included TFEB, identified a sub-cluster of genes, including *TFEB, GABARAP,* and *p62/SQSTM1.* That expression of *p62/SQSTM1, GABARAP,* and *TFEB* clusters together is significant and suggests potential co-regulation of these genes (Figure 3D). We identified a panel of genes that, like *TFEB,* shows impaired ATRA-induced expression in *TFEB*-depleted NB4 cells. The effect of TFEB depletion on ATRA regulation of the key autophagy genes, *p62/SQSTM1, GABARAP,* and *ATG16L1*, was confirmed by qRT-PCR (Figure 3D,E,F). The ATRA-mediated induction of p62/*SQSTM1* was attenuated in *TFEB*-knockdown cells, consistent with *p62/SQSTM1* being a direct TFEB target (Figure 3). *p62/SQSTM1* has a functional role in ATRA-mediated NB4 differentiation.[12] Other known ATRA-regulated autophagy genes include granulin, *GRN*, a gene encoding a glycoprotein with a role in inflammation that is highly expressed in myeloid cells (Figure 3C, highlighted).[40]

TFEB depletion reduces ATRA-mediated myeloid differentiation of APL cells

We next evaluated whether *TFEB* expression was required for ATRA-induced expression of the myeloid differentiation signature in APL cells by comparing vehicle and ATRA-treated control and TFEB-depleted cells (Supplemental Table 4B). Cufflinks RPKM values for these genes in *shScr-Ctrl*, *shScr-ATRA*, *shTFEB-Ctrl,* and *shTFEB-ATRA* cells were visualized using Treeview heatmaps (Figure 4A-B, Supplemental Table 4B). From our panel of 217 myeloid genes we identified clustered sub-networks of genes, suggesting potential co-regulation, that displayed ≥1.5-fold increases in transcript levels during ATRA treatment of non-transfected NB4 cells (Supplemental Table 2C). We used a 1.5-fold change cutoff for Figure 4A-B to detect statistically significant changes in myeloid gene expression related to ATRA and TFEB. We detected genes increased by ATRA, such as *ITGAM, ETS1, CEBPE, and TFE3* (Figure 4A), and genes decreased by ATRA, including *MYC, GATA2,* and *CEBPA* (Figure 4B). ATRA induced a ~40-fold increase in *ITGAM/CD11b* expression in *shScr* cells as compared to ~10-fold induction in *shTFEB* cells (Figure 4A and Supplemental Table 4B). We next tested whether this transcriptional phenotype that suggested impaired myeloid differentiation following depletion of TFEB expression was also evident by assessing the morphology of cells following ATRA treatment. ATRA-treated *shScr* cells at 48 hours displayed early morphologic signs of granulocyte differentiation (Figure 4C, upper panels). ATRA-treated *shTFEB* cells showed reduced differentiation, with a persistent immature phenotype (Figure 4C, lower panels, arrows).

We also validated expression of these differentiation markers, *ITGAM/CD11b*, *GCSFR,* and *CTSD,* by qRT-PCR. ATRA-treated *shTFEB* cells displayed less induction of each of these transcripts at 72 hours compared to ATRA-treated *shScr* cells ($p < 0.0001$) (Figure 4D,E,F). Similarly, ATRA induced a 9-fold increase in *CEBP*ε transcripts in *shScr* cells as compared to a ~6.5-fold increase in *shTFEB* cells (Figure 4A, Supplemental Table 4B). Conversely, the

ATRA-associated reduction in *GATA2* was greater in *shScr* (-10-fold) compared to the *shTFEB* cells (-5.8-fold) (Figure 4B, Supplemental Table 4B).[33] Depletion of *TFEB* also impaired ATRA-induced reduction of transcripts for transcription factors *CEBP*α and *MYC* (Figure 4B). We also noted lack of induction of *ETS1*, a transcription factor with documented roles in hematopoiesis, in the NB4 *shTFEB* cells (Figure 4A).[41]

Surface expression of *ITGAM/CD11b* protein was also examined by flow cytometry (Supplemental Figure S2). ATRA-induced differentiation is significantly reduced in the shTFEB cells compared to shScr controls ($p < 0.0001$).

These results show for the first time a major, functional role for TFEB in ATRA-induced myeloid differentiation-utilising gene, cell and morphological analysis in cell lines and primary patient samples. Importantly, the effects of *TFEB* knockdown on the expression of several myeloid differentiation genes are striking, placing these genes downstream of *TFEB*.

Effect of TFEB knockdown on autophagy

Our data thus far has suggested that ATRA-induced TFEB plays an important role in leukemic cell differentiation. We next evaluated whether the effects of TFEB were related to its regulation of autophagy. To do this, we initially compared autophagic flux in the shScr and shTFEB clones. Autophagic flux refers to the entire autophagy process, from sequestration to degradation. Autophagosome accumulation or an increase in autophagy markers may be a consequence of either increased autophagy initiation or a block in autophagosome turnover. Therefore, to differentiate between induction of autophagosomes and failure of turnover, cells were pre-treated with chloroquine to block lysosome function and autophagosome turnover. Any autophagosome accumulation beyond that observed with chloroquine alone is then attributed to enhanced autophagy initiation.

We examined the expression levels of LC3 I/II (autophagosome marker) in ATRA-treated cells, in the absence and presence of chloroquine (Figure 5). Analysis of LC3 II by Western blot

indicates increased LC3 II in the untreated shTFEB cells (lane 5) compared with shScr controls (lane 1), indicative of enhanced endogenous autophagy – despite TFEB silencing. This enhancement of endogenous autophagy is further evident in the presence of chloroquine (lane 3 versus lane 7), which blocks turnover of the endogenous autophagosomes. In the presence of ATRA alone, LC3 II levels were increased to a similar extent in both the scramble control and shTFEB cells, when compared to their own untreated controls. In the scramble control cells this ATRA-induced increase was further enhanced by chloroquine, indicative of autophagy flux. However no increase in flux was observed in the shTFEB clone (lanes 7 & 8). The levels of LC3 II in the combination-treated shTFEB cells are no greater than those observed with chloroquine alone. This is indicative of less initiation of autophagy by ATRA in the shTFEB clone.

Evidence for alternative autophagy

The previous LC3II blot indicated higher basal levels of LC3 II protein in the shTFEB clone (Figure 5). Therefore, despite TFEB knockdown there are still autophagosomes present, which also accumulate when the cells are treated with chloroquine. TFEB is only one of several transcription factors known to influence autophagy and alternative mechanisms of autophagy have been described, which do not need all of the components of autophagy initiation complexes. We therefore investigated whether there might be a TFEB independent / alternative autophagy present in these cells. One of these pathways is thought to originate at the Golgi and is disrupted by Brefeldin A (BFA), a golgi inhibitor.[42] We therefore examined whether BFA sensitive-autophagy might contribute to the autophagy present during differentiation.

For these experiments, we employed an additional marker of autophagy, Cyto-ID. This is a fluorescent dye which accumulates inside autophagosomes and enables the quantitation of autophagosomes by flow cytometry. We initially examined the effects of BFA on endogenous

levels of autophagy in the shScr and shTFEB clones. TFEB knockdown alone significantly increased Cyto-ID fluorescence, (black overlay) beyond scramble control (grey filled histogram) (*** p = 0.0009 internal bar graph), consistent with the enhanced levels of autophagosomes in the shTFEB clone noted in Figure 5. In addition, treatment of both scramble control (red overlay) (** p = 0.0073) and shTFEB (pink overlay) (*** p = 0.0001) cells with BFA inhibited endogenous autophagy to levels below untreated scramble controls (Figure 6A,i). Triplicate data are presented as mean fluorescence intensities, with each control normalised to one (Figure 6A,ii). These data suggest that the elevation of basal autophagy in the shTFEB cells is primarily due to BFA-sensitive/alternative autophagy.

To assess if ATRA-induced autophagy is also influenced by BFA we treated shScr and shTFEB cells with ATRA in the absence and presence of BFA (Figure 6B). In both the scramble control (i) and shTFEB (ii) cells the ATRA-induced increase in autophagosomes (red overlays) is significantly reduced in the presence of BFA (blue overlays) (*** $p < 0.0001$). In the shTFEB cells fluorescence levels are reduced to levels below those detected in untreated cells. These data were combined as triplicate mean fluorescence intensities, with each control normalized to one (Figure 6B,iii), highlighting the inhibitory effect that TFEB silencing has on ATRA-induced autophagy, an effect which is augmented by BFA treatment. Western blot analysis confirmed ATRA-mediated induction of autophagy/LC3II, in both the scramble and shTFEB clones, with lower levels of LC3 II induced in the shTFEB clone relative to its control. BFA reduced the levels of LC3 II in both, however it did not eliminate LC3 II accumulation in either (Figure 6C).

Effect of BFA on differentiation of shScr and shTFEB cells

To assess the involvement of BFA-dependent autophagy in differentiation we examined the effect of BFA on CD11b expression. As shown in Supplemental Figure S3 (i) BFA treatment reduced endogenous differentiation in both the shScr (red overlay) (*** p = 0.0007) and

shTFEB (pink overlay) (* $p = 0.010$) cells. (ii) Triplicate mean fluorescence intensities highlight the BFA-dependent inhibition of endogenous differentiation in both scramble and shTFEB cells. In addition, as shown in Supplemental Figure S4, ATRA-induced differentiation in the shScr (i) and shTFEB (ii) cells (red overlays) is significantly reduced by BFA (blue overlays) (*** $p < 0.0001$ and $p = 0.0004$, respectively). Triplicate data were combined as mean fluorescence intensities, with each control normalised to one (Supplemental Figure S4,iii). These data again highlight the effect of TFEB silencing on ATRA-induced differentiation, an effect that is further enhanced by BFA treatment. In this experiment we cannot distinguish between a reduction in surface CD11b due to inhibition of alternative autophagy or due to impaired Golgi trafficking. Future studies may wish to address this as soon as more selective inhibitors of alternative autophagy pathways become available.

Discussion

We and others have reported that ATRA induces autophagy in APL cells and that this autophagy contributes to granulocytic differentiation.[11-13,23] The mechanisms through which ATRA activates autophagy, however, have not been well characterized. Autophagy is mTOR-dependent, as mTOR inhibition with rapamycin increases autophagy and promotes PML-RAR degradation.[13] PU.1 binds at the promoter of the microtubule-associated protein 1S (*MAP1S*) gene, a positive regulator of autophagy, and MAP1S inhibition interferes with APL cell differentiation.[43] As PU.1 expression is suppressed in APL and restored by therapeutic levels of ATRA, this is a potential indirect mechanism of autophagy induction.[44] ATRA may also have a role in autophagosome maturation through redistribution of a cation-dependent mannose-6-phosphate receptor to the developing autophagosome, leading to vesicle acidification.[45] Building on our previous work, we assessed the transcriptional effects of ATRA on autophagy-related genes (Supplemental Table 3B). We found altered transcript levels of >80 autophagy-related genes following ATRA addition, opening avenues for further study of the crosstalk between retinoid signaling and autophagy. From this gene list we focused on the master autophagy regulator *TFEB* as a potential critical communicator between retinoid signaling and autophagy. Although previous studies have used microarray technology (*e.g.* GSE19201) to assess gene expression changes in APL cells following ATRA treatment, this is the first study to use unbiased, genome-wide approaches to examine the role of TFEB in ATRA-induced differentiation.

Two independent, published ChIP-seq analyses[7,31] show RARα and RNApol II recruitment to the *TFEB* locus, indicating that *TFEB* may be a direct retinoid receptor target (Figure 2A). We show that *TFEB* expression increases in NB4 cells treated with ATRA (Figure 2B). We also show *TFEB* induction in cultured primary human APL cells and in non-myeloid primary cells treated with ATRA (Figure 2D). *TFEB* expression is induced in murine hepatocytes by

overexpression of cyclic AMP response element–binding protein (CREB) and its partner, CRTC2.[46] Analysis of published liver ChIP-seq data showed CREB binding peaks within the *TFEB* gene locus[46,47] ATRA induces the activity of CRE-dependent transcription factors, offering a possible mechanism for secondary TFEB activation upon ATRA treatment.[48]

Studies of TFEB regulation to date have focused on post-translational modifications to the TFEB protein. Under normal cellular conditions TFEB is phosphorylated by mammalian target of rapamycin complex 1 (mTORC1), resulting in its binding with 14-3-3 proteins and sequestration in the cytoplasmic compartment.[22,49] Supporting the idea that mTORC1 is the primary regulator of the TFEB protein, nutrient deprivation leads to nuclear translocation of TFEB and increased expression of TFEB target genes.[49] Delineation of the cellular localization of the TFEB protein during ATRA-mediated APL cell differentiation is an area for further investigation. Functional depletion of TFEB in NB4 also impaired ATRA induction of the key autophagy associated genes *p62/SQSTM1, GABARAP,* and *ATG16L1* (Figure 3D,E,F). Our data suggest that TFEB is a key mediator of ATRA-induced autophagy processes during myeloid differentiation.

The large fold increase in *TFEB* mRNA during ATRA-mediated APL differentiation, along with our data that this induction is attenuated in differentiation-resistant NB4R cells (Figure 2C), led us to test for a functional role of TFEB in the APL cell differentiation process. Gene expression profiling by RNA-seq of *shTFEB* NB4 cells revealed a failure of these cells to activate the myeloid transcription program upon ATRA treatment, with impaired reductions in *GATA2, CEBPα* and *MYC* transcripts, as well as impaired induction of *PU.1* and *CEBPE*. Transcripts of *ITGAM* (*CD11b*), a commonly reported marker of myeloid differentiation, were also induced by ATRA to a lesser extent in *shTFEB* cells (Figure 4D). Similarly, ATRA induction of *GCSFR* and *CTSD* transcripts is impaired in *TFEB*-depleted NB4 cells. Our data convincingly show for the first time a major role for TFEB in the ATRA-mediated myeloid differentiation of APL cells.

One major function of TFEB is the coordination of autophagic flux by transcriptional regulation of the CLEAR network of genes encoding the machinery involved in autophagosome formation, cargo recognition, vacuolar fusion, and lysosomal degradation. Indeed, we confirm that *TFEB* knockdown alters the expression of downstream CLEAR network genes (Figure 3). As a protein degradation pathway, autophagy has been implicated in the degradation of the aggregate-prone PML-RARα oncoprotein, a process necessary for sustained therapeutic remissions in APL.[9,12,13] We previously showed that promoting autophagy can potentiate ATRA-mediated differentiation of the HL60-Diff-R cell line, a human AML line which does not harbor the PML-RARα oncoprotein and does not differentiate in response to ATRA treatment alone.[11] This finding suggests that autophagy plays a role in the cellular remodeling that occurs during differentiation and is not solely involved in oncoprotein elimination. Thus, TFEB induction may be critical in managing the considerable proteostatic stress of a differentiating cell.

Our analysis of LC3 II expression and autophagosome accumulation indicates an impairment in autophagic flux in shTFEB cells. This impairment in autophagy may be a key factor in the impairment of differentiation in shTFEB cells. The importance of autophagy in these cells is underscored by the fact that shTFEB cells can utilize an additional TFEB-independent pathway that can be inhibited by brefeldin A. This pathway is not just upregulated as a compensation in the shTFEB cells – it is also present in the shScr control cells – suggesting co-existence of autophagy pathways. This alternative pathway has previously been described in the context of leukemia cells. Wang *et al.* reported an alternative autophagic mechanism, in canonical autophagy-defective leukemia cells (Atg7-deleted K562 cells) – which was reversed by brefeldin A.[50]

This is the first study to indicate a potential role for alternative autophagy in differentiation. It is imperative to better understand the contribution of various autophagy pathways in order to effectively modulate it for the purposes of enhancing differentiation.

It is important to acknowledge that TFEB is a transcription factor that targets E-box (CANNTG) sequences on DNA and regulates the transcription of genes outside the CLEAR network. TFEB downstream-target genes involved in diverse cellular processes, including inflammation, metabolism and cell death, have been reported.[39] The effects of TFEB on differentiation could also be mediated by these genes, and indeed, a wider range of TFEB target genes may be identified in different cell contexts.

In conclusion, this study explores the communication between retinoid signaling and autophagy during APL cell differentiation. We identify *TFEB*, a master transcriptional regulator of autophagy and lysosomal biogenesis, as a direct retinoid target that is induced during ATRA-mediated differentiation. Importantly, we show that TFEB and autophagy, play a critical role in the myeloid differentiation process. Induction of TFEB may be of therapeutic benefit in broadening the use of differentiation therapy in ATRA-resistant, acute leukemias. The prospect of stimulating TFEB expression for therapeutic gain is an enticing one.

Acknowledgements

We thank the McKenna, Gudas, and Mongan laboratories for suggestions, and Daniel Stummer for assistance with manuscript preparation. This research was supported by the National Institutes of Health (CA043796) (LJG.) and by Weill Cornell funds. NO was funded by the Haematology Education and Research Trust (H.E.R.O), and Breakthrough Cancer Research (BCR), with unrestricted educational support from Pfizer, Merck, Sharp & Dohme, Bristol Myers Squibb, Novartis, and Amgen. The financial support of the University of Nottingham is gratefully acknowledged.

Authorship

Contributions: NO, TRO, MRC, DB, DMN, SLM, LJG, and NPM conceived, designed, and conducted the experiments; interpreted the results; and wrote the manuscript.

Correspondence: Nigel P. Mongan, Faculty of Medicine and Health Science, School of Veterinary Medicine and Science, University of Nottingham, LE12 5RD, Sutton Bonington, United Kingdom, e-mail: nigel.mongan@nottingham.ac.uk; Lorraine J. Gudas, Department of Pharmacology, Weill Cornell Medical College, 1300 York Avenue, New York, NY 10065, USA, e-mail: ljgudas@med.cornell.edu; and Sharon McKenna, Cork Cancer Research Centre & CancerResearch@UCC, Western Gateway Building, University College Cork, Cork, Ireland, s.mckenna@ucc.ie.

Conflict-of-interest disclosure: The authors declare no competing financial interests.

References

1. Tang XH, Gudas LJ. Retinoids, retinoic acid receptors, and cancer. *Annu Rev Pathol.* 2011;6:345-364.
2. Urvalek A, Laursen KB, Gudas LJ. The roles of retinoic Acid and retinoic Acid receptors in inducing epigenetic changes. *Subcell Biochem.* 2014;70:129-149.
3. Wang ZY, Chen Z. Acute promyelocytic leukemia: from highly fatal to highly curable. *Blood.* 2008;111(5):2505-2515.
4. Orfali N, McKenna SL, Cahill MR, Gudas LJ, Mongan NP. Retinoid receptor signaling and autophagy in acute promyelocytic leukemia. *Experimental cell research.* 2014;324(1):1-12.
5. Grignani F, De Matteis S, Nervi C, et al. Fusion proteins of the retinoic acid receptor-alpha recruit histone deacetylase in promyelocytic leukaemia. *Nature.* 1998;391(6669):815-818.
6. Collins SJ. Retinoic acid receptors, hematopoiesis and leukemogenesis. *Curr Opin Hematol.* 2008;15(4):346-351.
7. Martens JH, Brinkman AB, Simmer F, et al. PML-RARalpha/RXR Alters the Epigenetic Landscape in Acute Promyelocytic Leukemia. *Cancer Cell.* 2010;17(2):173-185.
8. Coombs CC, Tavakkoli M, Tallman MS. Acute promyelocytic leukemia: where did we start, where are we now, and the future. *Blood cancer journal.* 2015;5:e304.
9. Ablain J, Leiva M, Peres L, Fonsart J, Anthony E, de The H. Uncoupling RARA transcriptional activation and degradation clarifies the bases for APL response to therapies. *The Journal of experimental medicine.* 2013;210(4):647-653.
10. Trocoli A, Mathieu J, Priault M, et al. ATRA-induced upregulation of Beclin 1 prolongs the life span of differentiated acute promyelocytic leukemia cells. *Autophagy.* 2011;7(10):1108-1114.
11. Orfali N, O'Donovan TR, Nyhan MJ, et al. Induction of autophagy is a key component of all-trans-retinoic acid-induced differentiation in leukemia cells and a potential target for pharmacologic modulation. *Exp Hematol.* 2015;43(9):781-793 e782.
12. Wang Z, Cao L, Kang R, et al. Autophagy regulates myeloid cell differentiation by p62/SQSTM1-mediated degradation of PML-RARalpha oncoprotein. *Autophagy.* 2011;7(4):401-411.
13. Isakson P, Bjoras M, Boe SO, Simonsen A. Autophagy contributes to therapy-induced degradation of the PML/RARA oncoprotein. *Blood.* 2010;116(13):2324-2331.
14. Fullgrabe J, Klionsky DJ, Joseph B. The return of the nucleus: transcriptional and epigenetic control of autophagy. *Nature reviews Molecular cell biology.* 2014;15(1):65-74.

15. Choi AM, Ryter SW, Levine B. Autophagy in human health and disease. *N Engl J Med.* 2013;368(19):1845-1846.

16. Nakatogawa H, Suzuki K, Kamada Y, Ohsumi Y. Dynamics and diversity in autophagy mechanisms: lessons from yeast. *Nat Rev Mol Cell Biol.* 2009;10(7):458-467.

17. Birgisdottir AB, Lamark T, Johansen T. The LIR motif - crucial for selective autophagy. *J Cell Sci.* 2013;126(Pt 15):3237-3247.

18. Feng Y, He D, Yao Z, Klionsky DJ. The machinery of macroautophagy. *Cell Res.* 2014;24(1):24-41.

19. Rubinsztein DC, Marino G, Kroemer G. Autophagy and aging. *Cell.* 2011;146(5):682-695.

20. Cuervo AM. Cell biology. Autophagy's top chef. *Science.* 2011;332(6036):1392-1393.

21. Settembre C, Di Malta C, Polito VA, et al. TFEB links autophagy to lysosomal biogenesis. *Science.* 2011;332(6036):1429-1433.

22. Roczniak-Ferguson A, Petit CS, Froehlich F, et al. The transcription factor TFEB links mTORC1 signaling to transcriptional control of lysosome homeostasis. *Sci Signal.* 2012;5(228):ra42.

23. Humbert M, Mueller C, Fey MF, Tschan MP. Inhibition of damage-regulated autophagy modulator-1 (DRAM-1) impairs neutrophil differentiation of NB4 APL cells. *Leuk Res.* 2012;36(12):1552-1556.

24. Faria TN, Rivi R, Derguini F, Pandolfi PP, Gudas LJ. 4-Oxoretinol, a metabolite of retinol in the human promyelocytic leukemia cell line NB4, induces cell growth arrest and granulocytic differentiation. *Cancer Res.* 1998;58(9):2007-2013.

25. Nason-Burchenal K, Gandini D, Botto M, et al. Interferon augments PML and PML/RAR alpha expression in normal myeloid and acute promyelocytic cells and cooperates with all-trans retinoic acid to induce maturation of a retinoid-resistant promyelocytic cell line. *Blood.* 1996;88(10):3926-3936.

26. David KA, Mongan NP, Smith C, Gudas LJ, Nanus DM. Phase I trial of ATRA-IV and Depakote in patients with advanced solid tumor malignancies. *Cancer biology & therapy.* 2010;9(9):678-684.

27. Kashyap V, Ahmad S, Nilsson EM, et al. The lysine specific demethylase-1 (LSD1/KDM1A) regulates VEGF-A expression in prostate cancer. *Mol Oncol.* 2013.

28. Pfaffl MW. A new mathematical model for relative quantification in real-time RT-PCR. *Nucleic acids research.* 2001;29(9):e45.

29. Trapnell C, Roberts A, Goff L, et al. Differential gene and transcript expression analysis of RNA-seq experiments with TopHat and Cufflinks. *Nature protocols.* 2012;7(3):562-578.

30. Wang J, Duncan D, Shi Z, Zhang B. WEB-based GEne SeT AnaLysis Toolkit (WebGestalt): update 2013. *Nucleic acids research.* 2013;41(Web Server issue):W77-83.

31. Sotoca AM, Prange KH, Reijnders B, et al. The oncofusion protein FUS-ERG targets key hematopoietic regulators and modulates the all-trans retinoic acid signaling pathway in t(16;21) acute myeloid leukemia. *Oncogene.* 2016;35(15):1965-1976.

32. Rosenbauer F, Tenen DG. Transcription factors in myeloid development: balancing differentiation with transformation. *Nat Rev Immunol.* 2007;7(2):105-117.

33. Collin M, Dickinson R, Bigley V. Haematopoietic and immune defects associated with GATA2 mutation. *Br J Haematol.* 2015;169(2):173-187.

34. Hoffman B, Amanullah A, Shafarenko M, Liebermann DA. The proto-oncogene c-myc in hematopoietic development and leukemogenesis. *Oncogene.* 2002;21(21):3414-3421.

35. Tenen DG. Disruption of differentiation in human cancer: AML shows the way. *Nat Rev Cancer.* 2003;3(2):89-101.

36. Settembre C, Ballabio A. TFEB regulates autophagy: an integrated coordination of cellular degradation and recycling processes. *Autophagy.* 2011;7(11):1379-1381.

37. Lippai M, Low P. The role of the selective adaptor p62 and ubiquitin-like proteins in autophagy. *Biomed Res Int.* 2014;2014:832704.

38. Boorjian SA, Milowsky MI, Kaplan J, et al. Phase 1/2 clinical trial of interferon alpha2b and weekly liposome-encapsulated all-trans retinoic acid in patients with advanced renal cell carcinoma. *J Immunother (1997).* 2007;30(6):655-662.

39. Sardiello M, Palmieri M, di Ronza A, et al. A gene network regulating lysosomal biogenesis and function. *Science.* 2009;325(5939):473-477.

40. Ong CH, He Z, Kriazhev L, Shan X, Palfree RG, Bateman A. Regulation of progranulin expression in myeloid cells. *Am J Physiol Regul Integr Comp Physiol.* 2006;291(6):R1602-1612.

41. Zanocco-Marani T, Vignudelli T, Gemelli C, et al. Tfe3 expression is closely associated to macrophage terminal differentiation of human hematopoietic myeloid precursors. *Exp Cell Res.* 2006;312(20):4079-4089.

42. Cao Y, Zhang S, Yuan N, et al. Hierarchal Autophagic Divergence of Hematopoietic System. *The Journal of biological chemistry.* 2015;290(38):23050-23063.

43. Haimovici A, Brigger D, Torbett BE, Fey MF, Tschan MP. Induction of the autophagy-associated gene MAP1S via PU.1 supports APL differentiation. *Leuk Res.* 2014;38(9):1041-1047.

44. Mueller BU, Pabst T, Fos J, et al. ATRA resolves the differentiation block in t(15;17) acute myeloid leukemia by restoring PU.1 expression. *Blood.* 2006;107(8):3330-3338.

45. Rajawat Y, Hilioti Z, Bossis I. Retinoic acid induces autophagosome maturation through redistribution of the cation-independent mannose-6-phosphate receptor. *Antioxid Redox Signal.* 2011;14(11):2165-2177.

46. Seok S, Fu T, Choi SE, et al. Transcriptional regulation of autophagy by an FXR-CREB axis. *Nature.* 2014;516(7529):108-111.

47. Zhang X, Odom DT, Koo SH, et al. Genome-wide analysis of cAMP-response element binding protein occupancy, phosphorylation, and target gene activation in human tissues. *Proc Natl Acad Sci U S A.* 2005;102(12):4459-4464.

48. Saeki K, Saeki K, Yuo A. Distinct involvement of cAMP-response element-dependent transcriptions in functional and morphological maturation during retinoid-mediated human myeloid differentiation. *J Leukoc Biol.* 2003;73(5):673-681.

49. Martina JA, Chen Y, Gucek M, Puertollano R. MTORC1 functions as a transcriptional regulator of autophagy by preventing nuclear transport of TFEB. *Autophagy.* 2012;8(6):903-914.

50. Wang J, Fang Y, Yan L, et al. Erythroleukemia cells acquire an alternative mitophagy capability. *Scientific reports.* 2016;6:24641.

Figure legends

Figure 1. APL cells treated with ATRA activate a myeloid differentiation program. NB4 cells were seeded at 0.2 x 10^5 cells/mL and treated with either 1 μM ATRA or vehicle control for 72 hours. (A) Light microscopic morphological examination of control cells (upper panel) shows cells with large round nuclei and minimal cytoplasm consistent with an undifferentiated state (40x magnification). ATRA-treated cells (lower panel) show increased nuclear lobulation and decreased nuclear:cytoplasmic ratio indicative of granulocytic differentiation (40x magnification). (B) Gene expression changes induced by ATRA were examined using RNA sequencing (n=2). Shown here are the expression changes in a subset of genes associated with myeloid differentiation. All genes shown have a greater than 2-fold change in expression. Genes were grouped using Cluster software and a heatmap was generated with Treeview software. Critical myeloid transcription factors and markers of differentiation are highlighted. (D-H) Quantitative PCR validation of RNA sequencing data was performed. Measurements of *CD11b, C/EBPε, PIK3CD, GCSFR, CTSD* and the differentiation-associated autophagy gene, *GABARAP* mRNA levels are shown in ATRA-treated NB4 cells. Values are given as n-fold induction compared to untreated cells and normalized to housekeeping gene hPRT (n=6). t-test, **** $p < 0.0001$.

Figure 2. Effects of ATRA treatment on autophagy-related genes. (A) We interrogated a publicly available ChiP-seq datasets to examine retinoid signaling at the *TFEB* locus. An integrated genome viewer (IGV) depiction is shown of RARα and RNA-polymerase II (polII) binding at the *TFEB* gene following 24 hours after ATRA treatment in NB4 (grey) and TSU-1621-MT (black) cells. (B) (i-iii) NB4 cells were seeded at 0.2 x 10^5 cells/mL and treated with either 1μM ATRA or vehicle control. RNA was harvested at 72 hours. Measurement of *TFEB, p62* and *SIK3* mRNA levels by qPCR is shown (n=6). (C) (i-iii) Measurement of *TFEB, p62* and

SIK3 mRNA levels in differentiation-resistant NB4R cells seeded at 0.2 x 10^5 cells/mL and treated with 1μM ATRA for 72 hours (n=6). (D) (i-v) Mononuclear cells extracted from the bone marrow of a patient with APL were treated with ATRA in methylcellulose culture for 72 hours prior to RNA harvest. qPCR measurement of *TFEB, p62, SIK3, CD11b* and *PIK3CD* mRNA levels is shown (n=1). For all qPCR experiments, values are given as n-fold induction compared to untreated cells and normalized to housekeeping gene hPRT. Statistical significance determined with t-test, * $p < 0.05$, **** $p < 0.0001$.

Figure 3. Effects of TFEB knockdown on genes of the CLEAR network during APL cell differentiation. NB4 cells expressing non-targeting shRNA (shScr) or shRNA targeting TFEB (shTFEB) were seeded at 0.2 x 10^5 cells/mL and treated with either 1 μM ATRA or vehicle control. RNA was extracted at 72 hours. (A) Quantification of *TFEB* mRNA levels by qRT-PCR as validation of *TFEB* knockdown efficiency. We show that shTFEB impairs ATRA induction of *TFEB*. (B) RNA was sequenced in duplicate (n=2). Gene expression changes in shScr- and shTFEB-NB4 cells treated with ATRA were determined using Cuffdiff software. The Venn diagram depicts the cross-referencing of genes differentially expressed between ATRA-treated shScramble cells (yellow circle) and ATRA-treated shTFEB cells (purple circle). Genes outside the intersection are those affected by TFEB depletion. (C) A subset of genes from the CLEAR network with a greater than 1.5-fold change in expression following ATRA treatment underwent cluster analysis and are depicted here using a Treeview heatmap (legend provided). Quantification of SQSTMI/p62 (D), GABARAP (E) and ATG16L1 (F) mRNA levels by qRT-PCR. For all qPCR, values are given as n-fold induction compared to untreated cells and normalised to housekeeping gene hPRT (n=6). Statistical analysis was performed using ANOVA with Bonferroni's post hoc test, *** $p < 0.001$, **** $p < 0.0001$.

Figure 4. Effects of TFEB knockdown on ATRA-mediated APL cell differentiation. Using RNA sequencing, the expression of genes involved in myeloid differentiation was examined in NB4 cells expressing either non-targeting shRNA (shScr) or shRNA targeting TFEB (shTFEB) treated with ATRA for 72 hours (n=2). (A) Genes induced by ATRA are displayed following cluster analysis using Treeview software (legend provided). Only genes that display a greater than 1.5-fold change in expression in wild type NB4 cells are shown. Highlighted genes represent important myeloid transcription factors and markers of differentiation normally activated during differentiation but whose expression is reduced by TFEB depletion. (B) Genes whose expression is reduced by ATRA are shown. Highlighted genes represent important transcription factors that fail to be appropriately downregulated in shTFEB cells. (C) Quantification of CD11b mRNA levels by qPCR in shSCR and shTFEB cells following 72 hours of ATRA treatment. Values are given as n-fold induction compared to untreated cells and normalized to housekeeping gene hPRT (n=6). t-test, **** $p < 0.0001$. (D) Morphologic appearance of shSCR (upper panels) and shTFEB (lower panels) following 72 hours of ATRA treatment under light microscopy (40x magnification). Arrows depict persistent undifferentiated cells in TFEB-depleted cells.

Figure 5 ATRA-induced autophagy flux is impeded by TFEB knockdown. NB4 cells expressing non-targeting shRNA (shScr) or shRNA targeting TFEB (shTFEB) were seeded at 0.5×10^5 cells/mL. Cells were treated with ATRA alone (1 μM) for 72 hours, chloroquine alone (10 μM) for 72 hours or a combination of both, with chloroquine added 2 hours prior to the addition of ATRA. (i) Autophagic flux was assessed by Western blot analysis of LC3 II levels in shScr (lanes 1-4) or shTFEB cells (lanes 5-8), following treatment with ATRA (lanes 2 and 6), chloroquine (lanes 3 and 7) or a combination of both (lanes 4 and 8). An increase in LC3 II in scramble control cells treated with ATRA and chloroquine, beyond chloroquine alone is

indicative of flux. In the shTFEB clone however, flux is impeded – with no induction in LC3 II beyond that induced with chloroquine alone. (ii) All bands were quantified and normalised to β-actin. These data are presented as integrated intensities, with all bands normalised to untreated shScr cells (n=2).

Figure 6 Brefeldin A (BFA) inhibited endogenous and ATRA-induced autophagy in scramble control and TFEB knockdown cells. NB4 cells expressing non-targeting shRNA (shScr) or shRNA targeting TFEB (shTFEB) were seeded at 0.5 x 10^5 cells/mL. (A) (i) To confirm the effects of TFEB knockdown on endogenous autophagy, the Cyto-ID autophagy detection assay was used to measure autophagosome formation in shTFEB (black overlay) and shScr (grey histogram) cells. To assess the effects of BFA on endogenous levels of autophagy, cells were treated with BFA (10μM) for 24 hours – which reduced autophagy levels in both the shScr (red overlay) and shTFEB (pink overlay) cells. (ii) Data from three independent experiments is presented to the right as mean fluorescence intensities ± SEM with each control normalised to one (*** $p < 0.001$, ** $p < 0.01$). (B) The effect of BFA on ATRA-induced autophagy was assessed in (i) shScr and (ii) shTFEB cells. Cells were treated with ATRA (1 μM) for 72 hours, with BFA (10μM) added for the final 24 hours. BFA significantly reduced ATRA-induced autophagy (blue overlay) in both scramble control and shTFEB cells, when compared to ATRA alone (red overlays) – with a greater reduction in the shTFEB cells. Data from three independent experiments is presented as mean fluorescence intensities ± SEM within each panel (*** $p < 0.0001$). (iii) These data are combined and presented as triplicate mean fluorescence intensities, with each control normalised to one. (C) Autophagy was also assessed by Western blot analysis of LC3 II levels in shScr (lanes 1-4) or shTFEB cells (lanes 5-8), following treatment with ATRA alone (lanes 2 and 6), BFA alone (lanes 3 and 7) or a combination of both (lanes 4 and 8). An increase in LC3 II in ATRA-treated scramble

control and shTFEB cells was significantly reduced by BFA (lanes 4 & 8), yet not eliminated. All bands were quantified and normalised to β-actin. These data are presented as integrated intensities, with each band normalised to untreated shScr cells (n=2).

Supplemental Figure S1. Peripheral blood mononuclear cells (PBMCs) were obtained from patients with non-hematologic malignancy undergoing investigative in vivo ATRA therapy. qRT-PCR measurements of TFEB mRNA levels were performed on stored complementary DNA from these samples. Values are given as n-fold induction compared to untreated cells and normalized to housekeeping gene hPRT (n=3). Mann Whitney U test. ***p < 0.001.

Supplemental Figure S2. TFEB knockdown impedes ATRA-induced differentiation in NB4 cells. NB4 cells expressing non-targeting shRNA (shScr) or shRNA targeting TFEB (shTFEB) were seeded at 0.5 x 10^5 cells/mL and treated with either 1 μM ATRA or vehicle control for 72 hours. **(i)** Surface expression of CD11b was used to assess differentiation in untreated shScr (grey histogram), untreated shTFEB cells (black overlay) and in ATRA treated shScr (red overlay) and shTFEB (pink overlay) cells. **(ii)** Data from three independent experiments is presented to the right as mean fluorescence intensities ± SEM with each control normalised to one (*** $p < 0.0001$).

Supplemental Figure S3. Inhibition of Brefeldin A (BFA)-dependent autophagy reduced endogenous differentiation in scramble control and TFEB knockdown cells. NB4 cells expressing non-targeting shRNA (shScr) or shRNA targeting TFEB (shTFEB) were seeded at 0.5 x 10^5 cells/mL and treated with 10 μM BFA or vehicle control for 24 hours. (i) Surface CD11b expression was assessed. Basal levels of differentiation are elevated in the shTFEB cells (black overlay) when compared to scramble control (grey histogram). BFA reduced endogenous differentiation in both shScr (red overlay) and shTFEB (pink overlay) cells. (ii) Data from three independent experiments is presented to the right as mean fluorescence intensities ± SEM (*** $p < 0.001$ * $p < 0.01$).

Supplemental Figure S4. Inhibition of Brefeldin A (BFA)-dependent autophagy reduced ATRA-induced differentiation in scramble control and TFEB knockdown cells. NB4 cells expressing non-targeting shRNA (shScr) or shRNA targeting TFEB (shTFEB) were seeded at 0.5 x 10^5 cells/mL and treated with ATRA (1 μM) for 72 hours, with BFA (10 μM) added for the final 24 hours. Differentiation was assessed at day 3 by measurement of surface CD11b expression (n = 3). ATRA-induced differentiation (red overlays) was significantly reduced by BFA (blue overlays) in both the (i) shScr and (ii) shTFEB cells. Data from three independent experiments is presented as mean fluorescence intensities ± SEM within each panel (*** $p < 0.0005$). (iii) These data are combined and presented as triplicate mean fluorescence intensities, with each control normalised to one.

Supplemental Table 1

Lists of autophagy (A) and myeloid (B) genes examined.

Supplemental Table 2

A. Differential genes identified in vehicle and ATRA-treated NB4 cells.
B. Gene ontologies identified from differential expressed genes in ATRA-treated NB4 cells.
C. Expression of myeloid genes in ATRA-treated NB4 cells.
D. Comparison of expression of autophagy and ATRA-regulated myeloid-related genes in ATRA-treated NB4 cells.

Supplemental Table 3

A. ATRA-induced differential gene expression in NB4 cells transduced with non-gene targeting shRNA (shControl).
B. ATRA-induced differential gene expression in NB4 cells transduced with shRNA targeting *TFEB (shTFEB).*
C. Identification of ATRA-regulated TFEB target genes in NB4 cells.

Supplemental Table 4

A. Effect of *TFEB* depletion on ATRA regulation of the CLEAR network expression.
B. Effect of *TFEB* depletion on ATRA regulation of myeloid gene expression.

Figure 1.

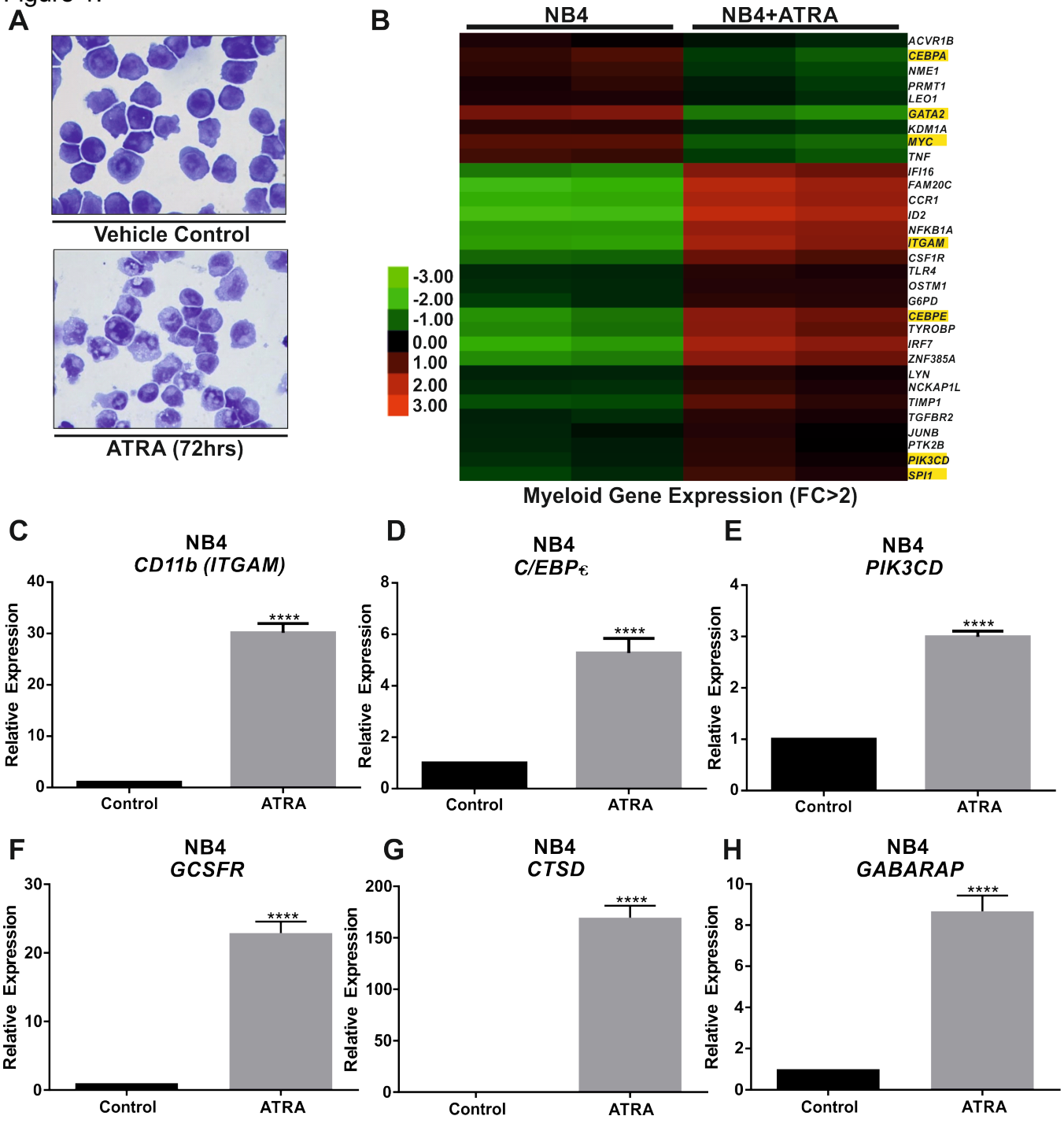
A
Vehicle Control
ATRA (72hrs)
B
NB4
NB4+ATRA
ACVR1B
CEBPA
NME1
PRMT1
LEO1
GATA2
KDM1A
MYC
TNF
IFI16
FAM20C
CCR1
ID2
NFKB1A
ITGAM
CSF1R
TLR4
OSTM1
G6PD
CEBPE
TYROBP
IRF7
ZNF385A
LYN
NCKAP1L
TIMP1
TGFBR2
JUNB
PTK2B
PIK3CD
SPI1
-3.00
-2.00
-1.00
0.00
1.00
2.00
3.00
Myeloid Gene Expression (FC>2)
C
NB4
CD11b (ITGAM)
D
NB4
C/EBPε
E
NB4
PIK3CD
F
NB4
GCSFR
G
NB4
CTSD
H
NB4
GABARAP
Relative Expression
Control
ATRA
****

Figure 2.

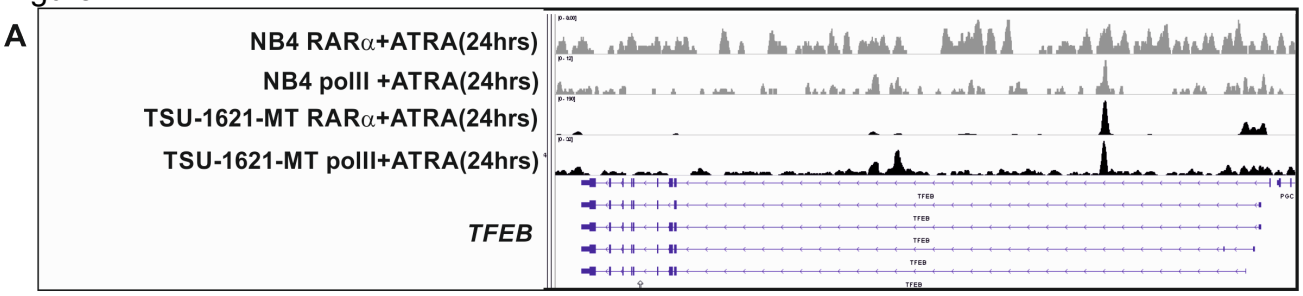
A
NB4 RARα+ATRA(24hrs)
NB4 polII +ATRA(24hrs)
TSU-1621-MT RARα+ATRA(24hrs)
TSU-1621-MT polII+ATRA(24hrs)
TFEB

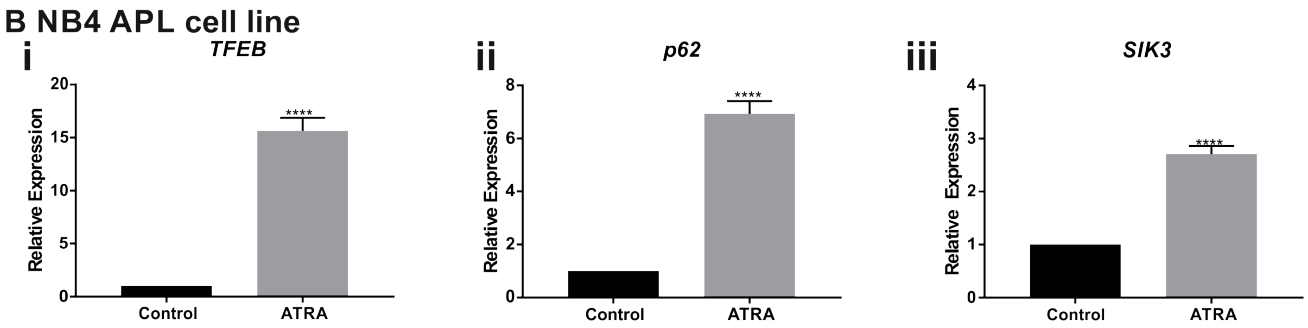
B NB4 APL cell line
i
TFEB
Relative Expression
Control
ATRA
ii
p62
iii
SIK3

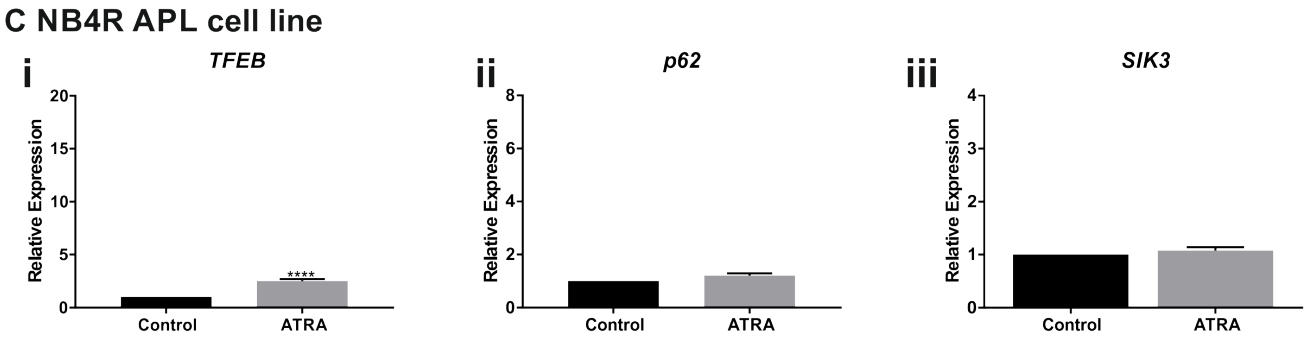
C NB4R APL cell line
i
TFEB
Relative Expression
Control
ATRA
ii
p62
iii
SIK3

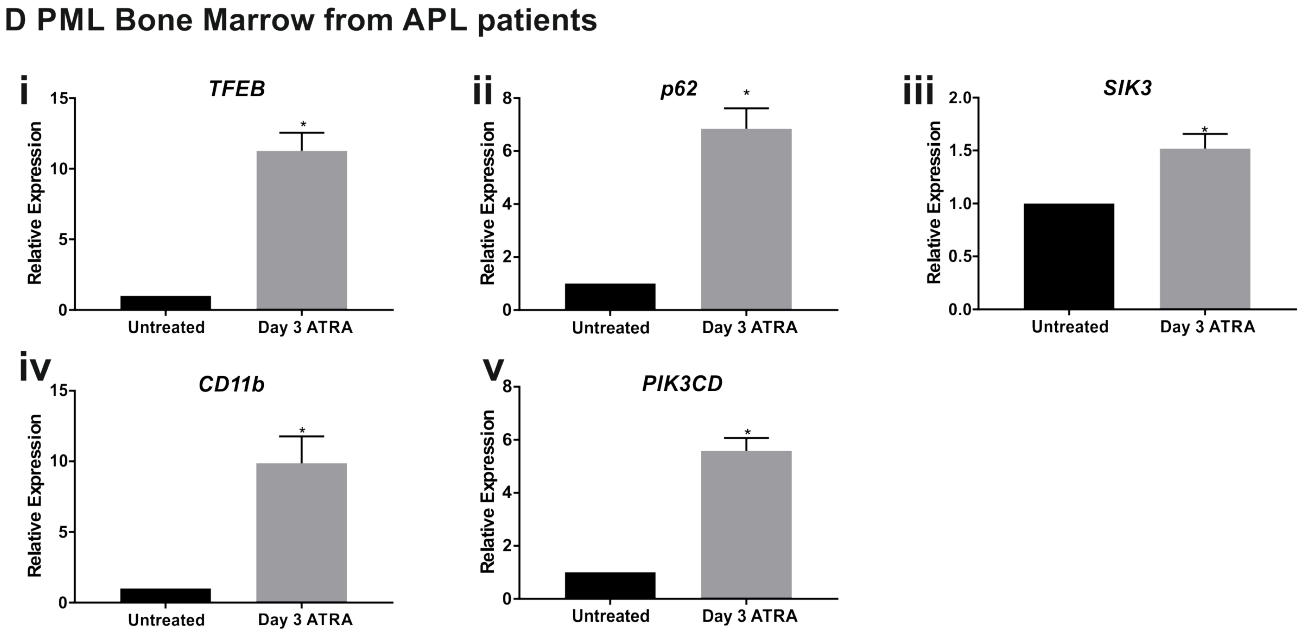
D PML Bone Marrow from APL patients
i
TFEB
Relative Expression
Untreated
Day 3 ATRA
ii
p62
iii
SIK3
iv
CD11b
v
PIK3CD

Figure 3.

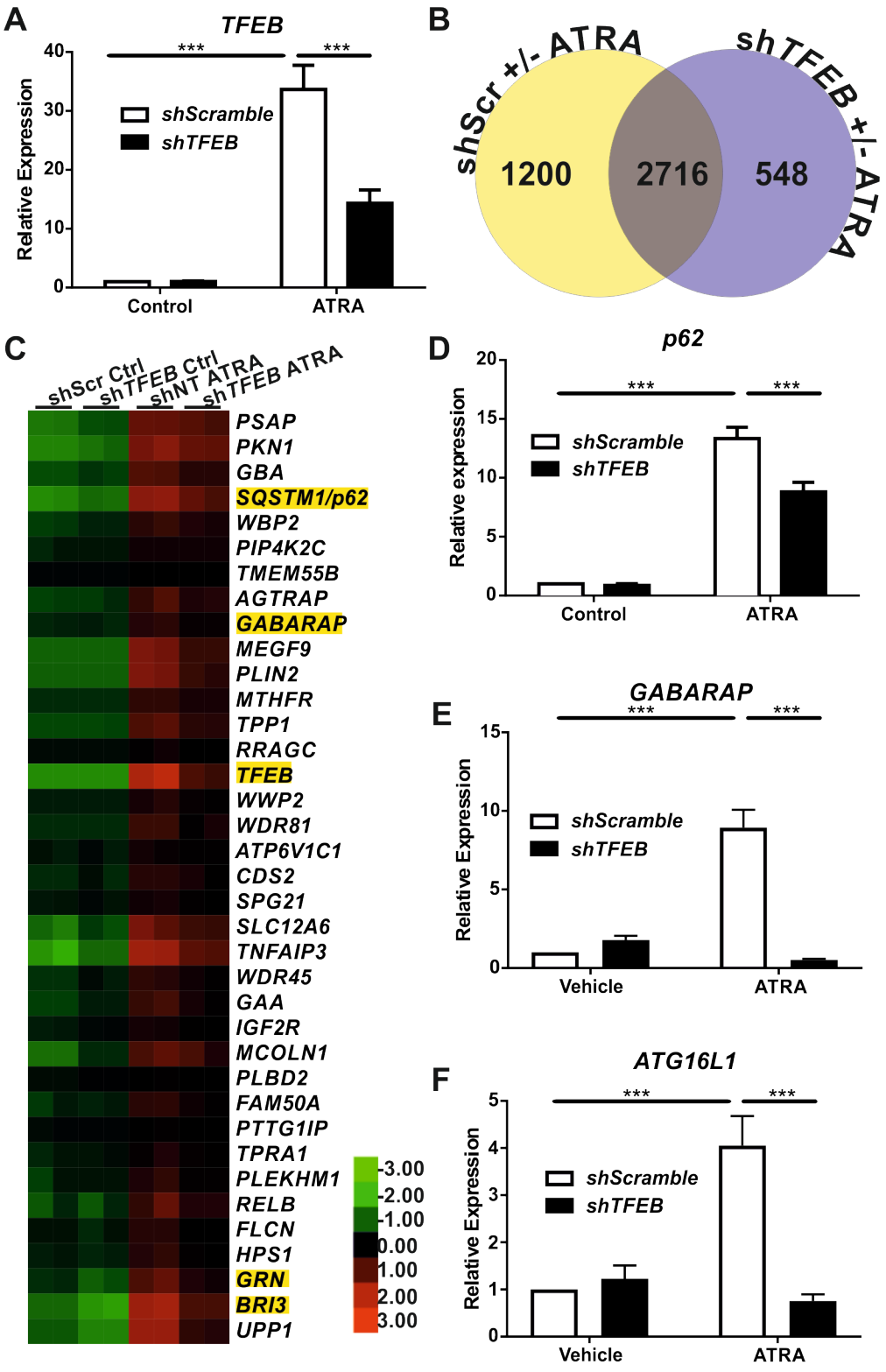
A
TFEB
***
***
Relative Expression
40
30
20
10
0
shScramble
shTFEB
Control
ATRA
B
shScr +/- ATRA
shTFEB +/- ATRA
1200
2716
548
C
shScr Ctrl
shTFEB Ctrl
shNT ATRA
shTFEB ATRA
PSAP
PKN1
GBA
SQSTM1/p62
WBP2
PIP4K2C
TMEM55B
AGTRAP
GABARAP
MEGF9
PLIN2
MTHFR
TPP1
RRAGC
TFEB
WWP2
WDR81
ATP6V1C1
CDS2
SPG21
SLC12A6
TNFAIP3
WDR45
GAA
IGF2R
MCOLN1
PLBD2
FAM50A
PTTG1IP
TPRA1
PLEKHM1
RELB
FLCN
HPS1
GRN
BRI3
UPP1
-3.00
-2.00
-1.00
0.00
1.00
2.00
3.00
D
p62
***
***
Relative expression
20
15
10
5
0
shScramble
shTFEB
Control
ATRA
E
GABARAP
***
***
Relative Expression
15
10
5
0
shScramble
shTFEB
Vehicle
ATRA
F
ATG16L1
***
***
Relative Expression
5
4
3
2
1
0
shScramble
shTFEB
Vehicle
ATRA

Figure 4.

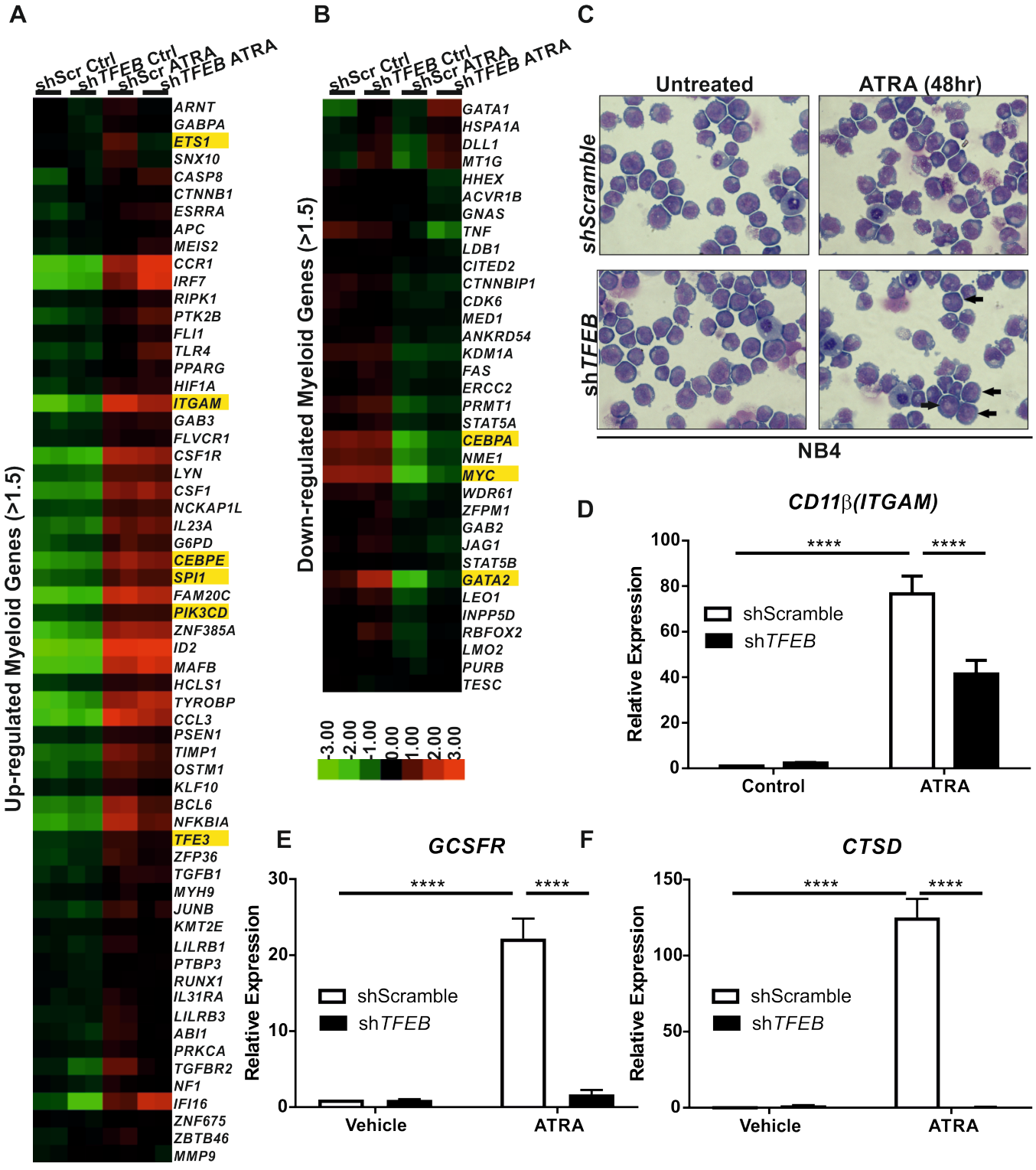
A
shScr Ctrl
shTFEB Ctrl
shScr ATRA
shTFEB ATRA
Up-regulated Myeloid Genes (>1.5)
ARNT
GABPA
ETS1
SNX10
CASP8
CTNNB1
ESRRA
APC
MEIS2
CCR1
IRF7
RIPK1
PTK2B
FLI1
TLR4
PPARG
HIF1A
ITGAM
GAB3
FLVCR1
CSF1R
LYN
CSF1
NCKAP1L
IL23A
G6PD
CEBPE
SPI1
FAM20C
PIK3CD
ZNF385A
ID2
MAFB
HCLS1
TYROBP
CCL3
PSEN1
TIMP1
OSTM1
KLF10
BCL6
NFKBIA
TFE3
ZFP36
TGFB1
MYH9
JUNB
KMT2E
LILRB1
PTBP3
RUNX1
IL31RA
LILRB3
ABI1
PRKCA
TGFBR2
NF1
IFI16
ZNF675
ZBTB46
MMP9
B
shScr Ctrl
shTFEB Ctrl
shScr ATRA
shTFEB ATRA
Down-regulated Myeloid Genes (>1.5)
GATA1
HSPA1A
DLL1
MT1G
HHEX
ACVR1B
GNAS
TNF
LDB1
CITED2
CTNNBIP1
CDK6
MED1
ANKRD54
KDM1A
FAS
ERCC2
PRMT1
STAT5A
CEBPA
NME1
MYC
WDR61
ZFPM1
GAB2
JAG1
STAT5B
GATA2
LEO1
INPP5D
RBFOX2
LMO2
PURB
TESC
-3.00
-2.00
-1.00
0.00
1.00
2.00
3.00
C
Untreated
ATRA (48hr)
shScramble
shTFEB
NB4
D
CD11β(ITGAM)
Relative Expression
100
80
60
40
20
0
****
****
shScramble
shTFEB
Control
ATRA
E
GCSFR
Relative Expression
30
20
10
0
****
****
shScramble
shTFEB
Vehicle
ATRA
F
CTSD
Relative Expression
150
100
50
0
****
****
shScramble
shTFEB
Vehicle
ATRA

Figure 5.

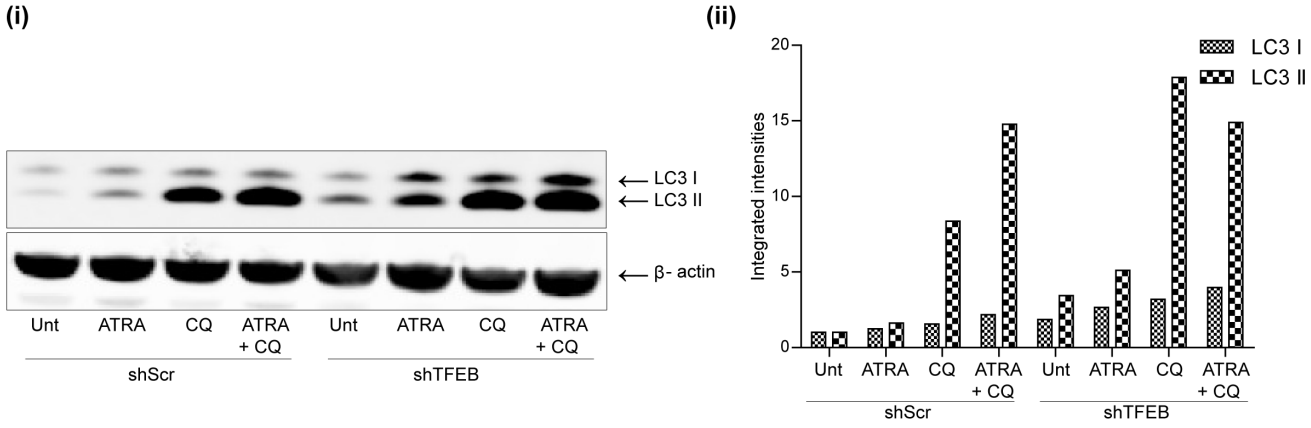
(i)
LC3 I
LC3 II
β- actin
Unt
ATRA
CQ
ATRA + CQ
Unt
ATRA
CQ
ATRA + CQ
shScr
shTFEB
(ii)
Integrated intensities
20
15
10
5
0
LC3 I
LC3 II
Unt
ATRA
CQ
ATRA + CQ
Unt
ATRA
CQ
ATRA + CQ
shScr
shTFEB

Figure 6.

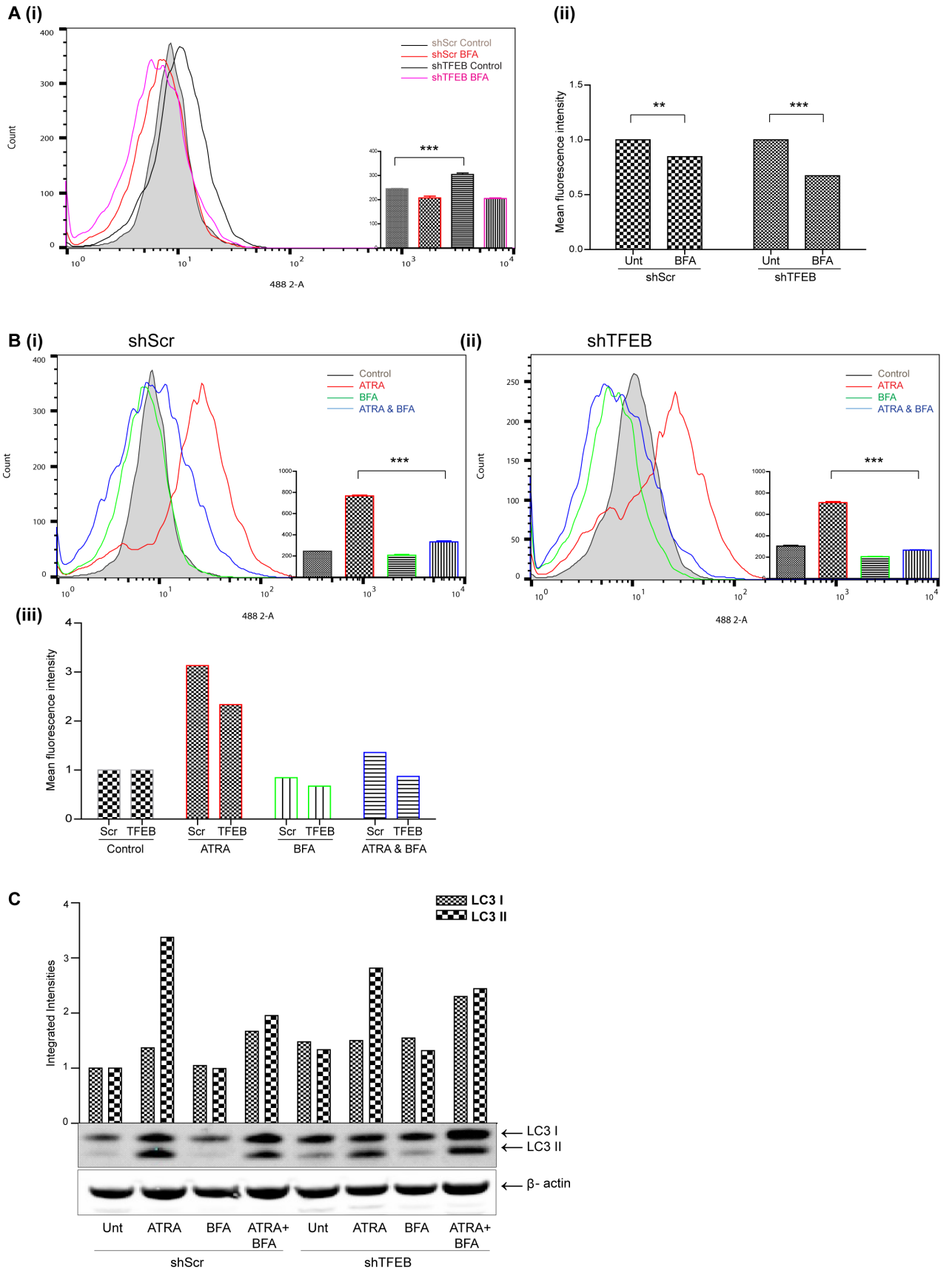
A (i)
shScr Control
shScr BFA
shTFEB Control
shTFEB BFA
Count
488 2-A
***
(ii)
Mean fluorescence intensity
**
***
Unt
BFA
shScr
shTFEB
B (i)
shScr
Control
ATRA
BFA
ATRA & BFA
(ii)
shTFEB
(iii)
Mean fluorescence intensity
Scr
TFEB
Control
ATRA
BFA
ATRA & BFA
C
LC3 I
LC3 II
Integrated Intensities
β- actin
Unt
ATRA
BFA
ATRA+ BFA
shScr
shTFEB

Supplemental Figure 1.

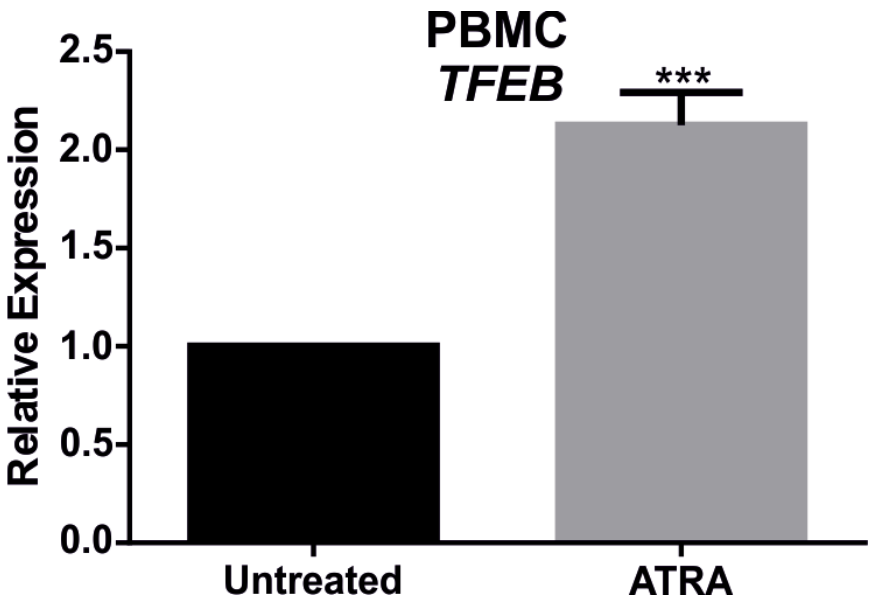

Supplemental Figure 2.

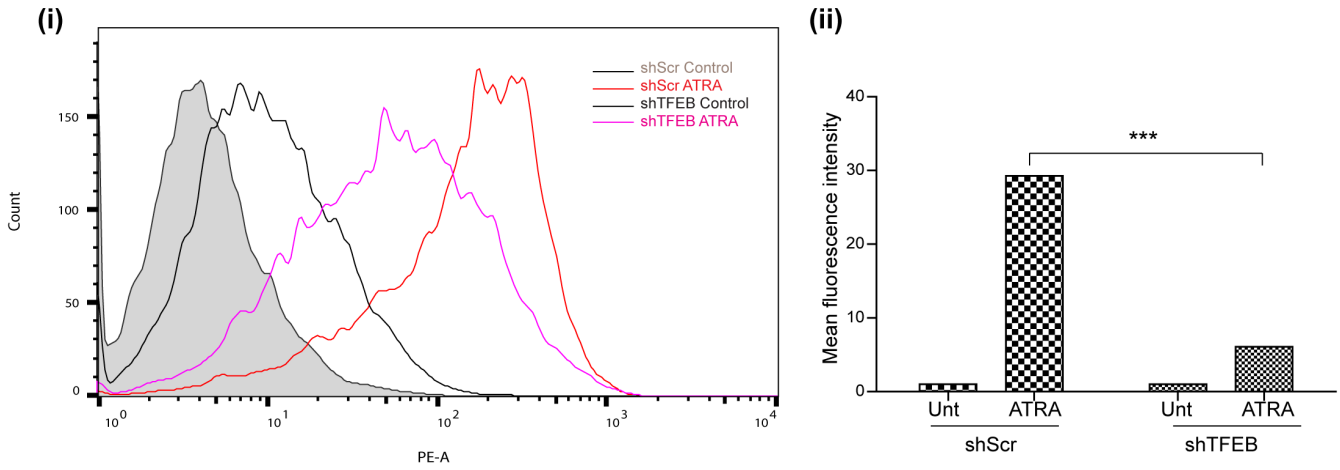

Supplemental Figure 3.

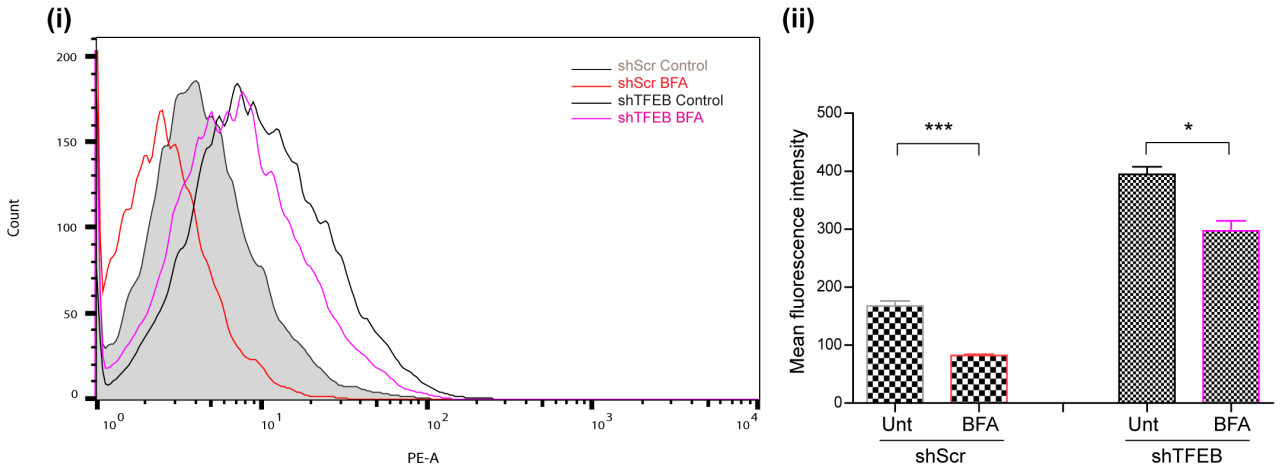

Supplemental Figure 4.